Energy & Buildings 244 (2021) 111037

Contents lists available at ScienceDirect

Energy & Buildings

journal homepage: www.elsevier.com/locate/enb

Evaluation of sustainable strategies and design solutions at high-latitude urban settlements to enhance outdoor thermal comfort

J. Brozovsky [a,*], S. Corio [b], N. Gaitani [a], A. Gustavsen [a]

[a] Department of Architecture and Technology, Faculty for Architecture and Design, NTNU – Norwegian University of Science and Technology, Høgskoleringen 1, 7491 Trondheim, Norway
[b] Department of Civil, Chemical and Environmental Engineering (DICCA), University of Genoa, 16145 Genoa, Italy

ARTICLE INFO

Article history:
Received 10 April 2020
Revised 21 March 2021
Accepted 15 April 2021
Available online 22 April 2021

Keywords:
Urban microclimate
Cold climate
Outdoor thermal comfort
Numerical analysis
Validation study

ABSTRACT

Driven by the necessity to design resilient and prosperous cities and to counteract the impacts of climate change, this study aims to shed light on the interactions between microclimate, urban built environment, and the outdoor thermal comfort (OTC) conditions at a university campus in Trondheim, Norway. This paper calls into question up to which degree four typical microclimatic design solutions can enhance OTC in high-latitude areas which are generally characterized by strong seasonal variability in meteorological conditions, particularly in solar radiation. An on-site measurement campaign in autumn 2019 for the validation of numerical simulations with ENVI-met were carried out. Solar access proved to be the key parameter to improve OTC by a Predicted Mean Vote of up to 1.0 in the investigated climatic situation. Moreover, wind sheltering resulted in an increase of OTC, although not as pronounced and on a smaller spatial scale. Changing the buildings' surface material resulted in no significant changes in microclimatic conditionsAt a higher wind speed (8 m/s), wind sheltering becomes more effective in improving OTC than solar access. This study underlines the importance of microclimatic assessments in order to understand the effect of different interventions with the urban environment on OTC at high-latitude urban settlements.

1. Introduction

Already in the 1830s, it was discovered that a city – London in this case – had a distinctly different climate than its rural surroundings [1]. Driven by the necessity for designing better cities and, especially nowadays, to counteract the observed and projected impacts of climate change and rapidly growing city populations worldwide [2,3], a great number of publications on urban climatology (UC) have been published since then. UC brings together many different disciplines such as meteorology, climatology, air pollution science, architecture, building engineering, physics, urban design, biometeorology, social sciences, etc. [4].

Undoubtedly, one of the most documented topics in urban climate research is the urban heat island (UHI) effect which describes the observed higher temperatures in urban areas by several degrees compared to the surrounding rural areas [5]. The UHI phenomenon has been reported to occur in urban areas of nearly any size and across all climate zones [6]. As the overheating of cities pose a serious threat to people's health [7–10] while at the same time increasing the cooling energy demand in buildings [11], research studies have primarily been aiming to mitigate the adverse effects of the UHI. This has been mainly addressed by studying the influence of urban trees and parks, e.g. [12–18], green roofs and facades, e.g. [13,19–22], water bodies, e.g. [19], the albedo of surfaces, e.g. [20–26], or smart materials, e.g. [27,28].

Even in cold-climate cities as defined by the Köppen-Geiger climate classification system, measures need to be taken to shield the urban areas from elevated temperatures. This was highlighted for example in Montreal [27,28] and Toronto [29] in Canada, as well as in Columbus in Ohio, USA [30]. However, the overall effect of the UHI on a city's energy use was found to be positive in some cases, e.g. in the North of the USA [31] or large Russian cities [32], meaning that the heating energy savings in winter surpass the cooling energy increase during the summer months.

The most commonly reported differences in air temperature between a city and its rural surroundings (the UHI-magnitude) over time are about 1–3 K in cold climate locations. The highest magnitudes were frequently reported during anticyclonic and calm weather conditions [33–35], mostly during the night [36–38] and

* Corresponding author.
E-mail address: johannes.brozovsky@ntnu.no (J. Brozovsky).

https://doi.org/10.1016/j.enbuild.2021.111037
0378-7788/

either in winter [39–41] or summer [38,42,43]. High-latitude areas experience a more pronounced seasonal variability in meteorological conditions compared to mid- or low-latitude areas [44]. In winter and spring, snow on the ground reflects most of the incident solar radiation during the short days due to a higher surface albedo [45]. In these regions, the anthropogenic heat release, related to space-heating and vehicle traffic, was identified as a major contributor to the UHI. Thus, the so-called urban self-heating is strongly linked to fuel use [36,46–49].

In the history of UC, among a variety of methodological approaches, the focus has been mainly in the careful recording and analysis of observations and field measurements until the 1960 s [4]. Nevertheless, over the last two decades, numerical analyses as a method to supplement the experimental investigations in urban studies have received a lot of attention [4,50]. However, they have primarily been carried out in warm and temperate climate regions [50]. Considering that there are more than 25 million people living above 60° N, research carried out in the high-latitude and cold-climate regions are extremely valuable. Local factors like an increasing population and ongoing urbanization [51–53] put increasing pressure on the circumpolar region as well as global ones like the increasing exploitation of resources in the more and more ice- and permafrost-free and thus accessible North [54]. This contributes to the steadily increasing global greenhouse gas emissions [55]. Having in mind that the arctic region is particularly vulnerable to the effects of climate change as it warms more rapidly than the global mean, research in these regions is much-needed [56].

Many publications stress the necessity of improving the design and the climate resilience of cities and their outdoor environment to provide comfortable spaces that invite people to spend time outdoors or that promote soft mobility, regardless of their climate, e.g. [11,57,58]. Human comfort (“the pleasant feeling of being physically or mentally free from pain or suffering” [59]) and well-being (“feeling healthy and happy” [59]) are terms frequently used when investigating the environmental quality in cities and the people’s perception. An experiment in an urban park in Xi’an, China by Xu et al. [60] suggests that human comfort and thermal sensation are strongly connected. In winter conditions, they identified solar radiation as the most important aspect, followed by air temperature and relative humidity. Wind was reported to be the least important aspect. The authors also highlighted that human perception of the environment was affected by psychological factors, supporting the physical and mental characteristics of comfort and well-being. Another survey by Liu et al. [61] underlined that air temperature is the most important microclimatic parameter in public urban squares. Thermal radiation was identified as the second most important one. In winter, however, when temperatures are always low, the authors observed the relative importance of solar radiation to increase and that of air temperature to decrease. In other words, solar radiation contributed more to outdoor thermal comfort than the air temperature. An increment in wind speed was reported to cause the outdoor neutral air temperature (i.e. the temperature at which the thermal sensation vote would be neutral) to increase, while thermal radiation had the opposite effect. An increase in humidity elevated the outdoor neutral air temperature in spring and autumn while showing contrary behavior in summer and winter. Similar results were obtained by Chen et al. [62] who investigated thermal sensation and comfort evaluation methods in Harbin, China. There, air temperature and solar radiation were found to be most influential for the thermal sensation in Harbin.

Nikolopoulou and Lykoudis [63] analyzed the data obtained from microclimatic and human monitoring of about 10.000 interviews across five different countries in Europe. They proved the strong relationship between microclimatic and human comfort conditions with air temperature and solar radiation as the most important parameters. High wind speeds furthermore amplified the feeling of discomfort. Only at high temperatures, the elevated wind speed was identified as desired. The authors attributed minor importance to relative humidity as people cannot judge these changes unless the humidity is particularly high or low. Their analysis revealed that people tend to adapt more easily to heat than to cold and that both physical and psychological adaptation is taking place.

Yang et al. [64] performed a field survey with structured interviews and microclimatic measurements in an urban park in the subarctic city of Umeå in Sweden. About half of the interviewed people expressed their preference to higher solar radiation even at a thermal sensation of “slightly warm”. Since lower wind speeds together with exposure to sunshine can improve the thermal sensation of people, they suggested a curved terrain to decrease wind without providing shade in urban outdoor environments, such as parks in the subarctic or arctic climate.

A questionnaire survey at public spaces in Montreal, Canada was analyzed by Stathopoulos et al. [65] for the development of an overall comfort index. The study revealed that Montreal’s citizens desire higher air temperatures and solar radiation but lower wind speed and relative humidity during spring and autumn, regardless of the actual weather conditions.

Lai et al. [66] conducted a survey in the city of Tianjin in northern China. Along with the previously mentioned studies, people preferred lower wind speed and higher solar radiation at low air temperatures and vice versa at high air temperatures. People were able to adapt to warm temperatures by changing their clothing and activity levels. At temperatures above 30 °C, people were not able to further adapt to the environment.

In their review of outdoor thermal comfort (OTC) and outdoor activities, Chen and Ng [67] stressed the importance of outdoor spaces in promoting the quality of life and livability in cities. As people most commonly interact with each other and the physical amenities in urban spaces, like street furniture, kiosk stands, etc., the use and the quality of outdoor spaces is not only determined by the “state of body” but also by the “state of mind”. Therefore, they suggested that the perception of thermal comfort should be assessed on four different levels; physical, physiological, psychological and social/behavioral.

ENVI-met is a frequently used tool to assess thermal comfort in outdoor spaces [68–71] and has also been used to assess OTC in cold climate conditions, e.g. Toronto, Canada [72,73]. Most commonly, however, the summerly OTC and mitigation strategies in the context of heatwaves and the UHI are investigated. Numerical studies dealing with OTC in the transitional seasons or winter in high-latitude locations, are scarce. In a paper by Gatto et al. [74], the impact of urban vegetation on OTC was investigated in winter conditions in Lahti, Finland by using ENVI-Met. They found that urban vegetation generally decreases the mean radiant temperature in a neighbourhood, not only close to the vegetation. On the other hand, local improvements of OTC were reported from urban vegetation through lower wind velocities, although very close to the trees, shading led to strongly decreased OTC.

To form a better view of the microclimatic considerations for outdoor spaces in cold climate regions and to assess how different strategies may improve OTC conditions in autumn conditions, four alternative design strategies for the thermal comfort improvement of NTNU campus in Norway were considered, simulated and evaluated. The paper is divided into five sections. The second section provides the geographic and climatic context of the study area. In the third section, the applied methodology and the validation process are presented along with the investigated solution strategies. The results and the discussion follow in Section 4. The conclusions are drawn in Section 5.

2. Study area and climatic context

This study was carried out at the Norwegian University of Science and Technology (NTNU) which is located on a hill near the city center of Trondheim (63.4° N, 10.4° E). Trondheim is Norway's third-largest city with close to 200.000 inhabitants and is situated at a large fjord in Central Norway. NTNU's campus (called Gløshaugen) is 0.23 km^2 and lies at an altitude between 38 and 49 m above sea level (see Fig. 1). Due to the integration of another separated campus to Gløshaugen, the study area is undergoing a large redevelopment process until 2027. Step-by-step, 90.000 m^2 of buildings will be added to the area, and about 45.000 m^2 of existing buildings are to be refurbished.

According to the Köppen-Geiger climate classification system Trondheim's climate is oceanic (Dfb), but closely borders continental, subpolar and subarctic climates [75]. From November to March, moderate snowfall mixed with milder weather patterns and rain is common. The annual mean temperature is 4.8 °C (1961–1990), summers are relatively short, and winters are long and cool (see Fig. 2). However, due to climate change, temperatures in the arctic and subarctic regions have been rising, so that the Norwegian average annual temperature of the last 10 years from 2009 to 2018 has been 1.1 °C higher than the long-term mean from 1900 to 2018 [76]. In Trondheim, the mean annual temperature from 2009 to 2018 was 6.0 °C which is 1.2 °C above the average temperature of the norm period from 1961 to 1990 [76]. The monthly average of relative humidity in the period from 2009 to 2018 is highest in September with 78.2%, while in May, it is lowest with 67.6%. It can be also seen in Fig. 2 that the windiest month is March with 3.0 m/s, while July and August both show the lowest average wind speed of 2.1 m/s for the period from 2009 to 2018. Considering the monthly averages of global horizontal radiation, the differences are much more pronounced on a monthly basis. While in July 17.5 MJ/m^2 have been recorded on average, in December it is only 0.2 MJ/m^2 [76].

These relatively pronounced differences are caused by the proximity to the Arctic Circle that leads to quite short days in winter (sunrise at 10:01 and sunset at 14:31 local time on 21st December) and relatively long days in summer (sunrise at 03:02 and sunset at 23:37 local time on 21st June). Consequently, the sun elevation angles throughout the year are relatively low, reaching 50.0° at the summer solstice and only 3.3° at the winter solstice (see Table 1). For comparison, the sun elevation angles of Toronto, Canada, a city located in the same Köppen-Geiger climate region (Dfb) are 69.8° and 22.9° at the solstices, respectively. Such low elevations, like in the case of Trondheim, impact the solar access in street canyons of urban areas significantly.

To the North and Northwest, the campus is embedded into a park-like surrounding. To the East, South, and Southwest, the campus borders suburban residential areas with predominately single-family homes. Due to computational limitations in the numerical model size, which will be explained in the next chapter, only the northern part of the campus is used for the investigation. It was selected as it is the busiest and most vibrant outdoor space on campus.

The main connection route between the buildings, and a space frequently used for activities of any kind, is "Stripa", a North-South oriented pedestrian zone, lined by trees and largely surrounded by buildings in the West, North and East, and open to the South (see also Fig. 3). There are three entrances to Stripa, one in the North, one in the West and one in the South. This area represents the most-frequented on campus. Here, students and staff tend to eat their lunch outside during nice weather, change classrooms or just go out to get some fresh air at around 12:00 local time. The results of our study should help to determine how thermal comfort at this time of the day can be enhanced, in order to promote these activities and extend the periods in which acceptable outdoor conditions allow for them.

3. Methodology

The methodology used in this study is twofold: (i) field measurements and (ii) numerical simulations. Punctual field measurements of microclimatic parameters in the area of interest provided the necessary data to validate the numerical simulation model of the campus. That was an imperative step to confirm that the accuracy of the model is sufficient for the intended use [77,78]. The numerical simulations were carried out with ENVI-met v. 4.4, a three-dimensional non-hydrostatic software model for the surface-plant-air interaction [79] that is broadly used for the analysis of design impacts on the local environment, the specification of materials, and the usage of vegetation in a different configuration.

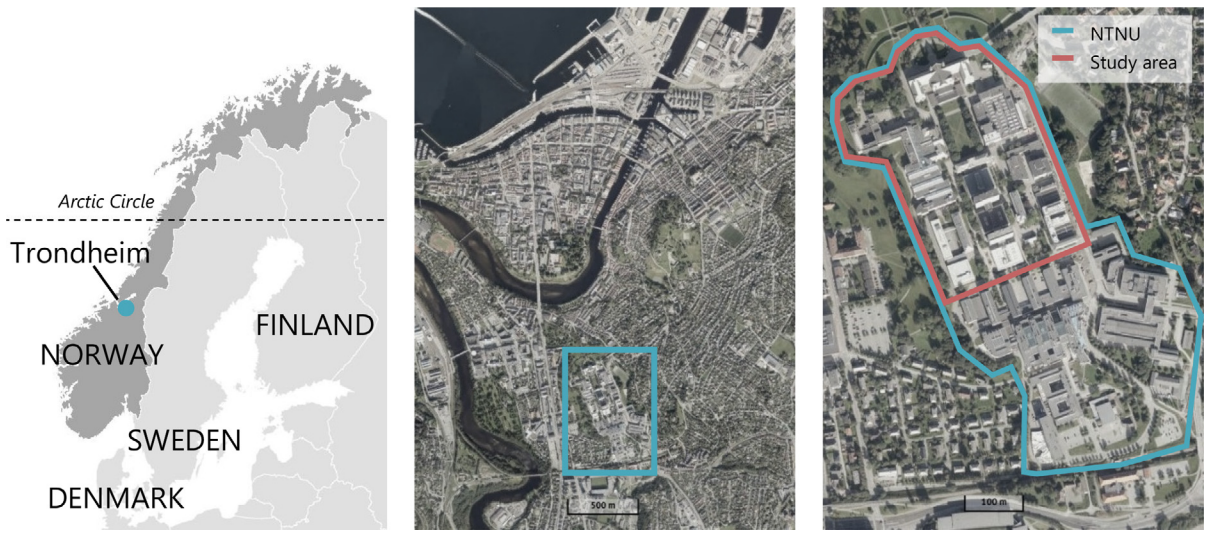

Fig. 1. Location of the study area and NTNU within Norway and Trondheim (aerial photographs from the Norwegian Mapping Authority www.kartverket.no).

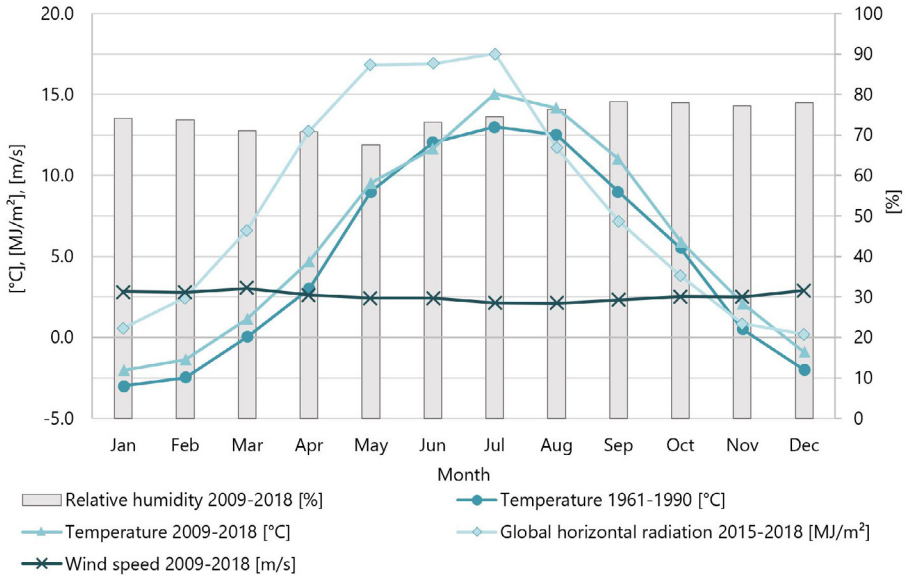

Fig. 2. Monthly averages of temperature, humidity and wind speed for Trondheim's weather station in Voll and average daily global horizontal radiation for each month for Gløshaugen campus [76].

Table 1
Sun elevation angles for different dates in Toronto, Canada and Trondheim, Norway.

Date	Max. sun elevation angle	
	Toronto, Canada (43.6° N)	Trondheim, Norway (63.4° N)
21.03. (vernal equinox)	47.0°	27.1°
21.06. (summer solstice)	69.8°	50.0°
23.09. (autumnal equinox)	45.9°	26.2°
20.10. (investigated day in this study)	35.7°	16.0°
21.12. (winter solstice)	22.9°	3.3°

Fig. 3. Stripa, seen from the South, during a sunny morning in autumn.

3.1. Measurement campaign

This study contains data collected from two different kinds of field measurements: (i) meteorological recordings and (ii) infrared (IR) thermography. For this study, measurements of one fixed weather station and four mobile weather stations were used (see Fig. 4). Fig. 5 shows photos of buildings in the different building categories on site. The fixed weather station of the campus, operated by the Dept. of Energy and Process Engineering, is located 10 m above the roof of the Varmeteknisk Laboratorium (VATL), 28 m above ground level. In this article, it will be further referred to as the reference weather station (RWS). The experimental data were obtained during a 4-week measurement campaign in autumn 2019 (from 27th September to 25th October) from four new on-site weather stations, mounted on tripods in 3 m height at different locations around the campus (see Fig. 6). A description of the used measurement equipment is given in Table 2. Furthermore, an H21-USB data logger was used to record data at a frequency of 0.1 Hz.

The conditions for the validation process were obtained on October 20th, 2019. On this day, a light breeze and clear sky conditions prevailed, with an average wind speed of 2.22 m/s, measured at the reference weather station on the VATL building. This day can be regarded as a typical, sunny autumn day in Trondheim. As mentioned earlier, IR thermography was used to obtain surface temperatures in addition to the meteorological measurements. Thermal images were taken for selected building surfaces. At designated locations, ground measurements were taken that include asphalted, paved and vegetated (grass) surfaces (see Fig. 4 and Fig. 5).

ENVI-met v. 4.4.2 was used to create a numerical model of the study area. ENVI-met simulation software incorporates the interactions between the atmosphere, materials, vegetation, radiation and the buildings to assess the urban environment [79]. This software was chosen because it is the most widely evaluated microclimate model available at present. Even though it is mostly used in temperate or warm climate conditions to evaluate measures for counteracting the UHI, e.g. [26,80–85], it can handle lower and below-zero temperature values as well. However, the used version did not permit to include snow on the ground and building surfaces which was found to affect the microclimate in cities [43,86], nor any form of precipitation. Within this limitation, simulations were performed only for dry weather conditions.

3.1.1. Computational domain geometry

For determining the positions of the different surface and vegetation cover types in the 3D model (Fig. 7), maps and aerial photographs provided by the Norwegian Mapping Authority (www.kartverket.no) from 2018 were used. On-site inspections provided

Fig. 4. Schematic site plan of the study area.

Fig. 5. Examples of the different building categories in the study area.

specific characteristics of the buildings, materials, and vegetation, including size and species. The created computational domain has the dimensions of 416 × 400 × 94.5 m^3 and was discretized into 104 × 100 × 32 grid cells, resulting in a 4-m grid in the horizontal directions, and a 3-m grid in the vertical. The lowest grid cell is subdivided into five cells with 0.6 m height respectively. According to the ENVI-met guidelines, the domain was modeled to be more than twice the height of the highest building (SB towers' height: 46 m, or 13 floors) and the horizontal distance to the model boundaries was larger than the closest building's height.

Fig. 6. Weather station B on a grass patch.Numerical model.

Initially, no computational nesting grids were added around the "normal" (visible) domain.

3.1.2. Materials and vegetation

In the area of interest, the ground surface types can be expressed by three main types: (i) grass, (ii) asphalt, and (iii) concrete pavement. Soil maps [87] of the region indicated a distinct clay content in the modeled area which matched the default soil profile (*sandy loam*) in ENVI-met. This profile was used below the buildings and the vegetative elements like grass, hedges, and trees. For the impermeable surfaces (ii) and (iii), the ENVI-met library entries *Asphalt Road* and *Pavement (Concrete), used/dirty* were employed [88].

Resulting from the park-like environment in which NTNU campus is embedded, green spaces, trees, shrubs, and hedges are common features in the study area. The amount of different sizes, species, individual peculiarities and the large number of elements necessitated a simplification of the model. Hence, the model was limited to three tree species, two hedge types and one grass type. The selected tree species were the most common tree types at the study site: (i) *Norway Maple* (modeled 10, 15 and 20 m tall), *Larch* (20 m) and *Scots Pine* (5 and 10 m). The seasonality of the foliation was considered by adapting the leaf area density (LAD) of the trees with a scaling factor. As the trees already started to defoliate, the scaling factor of 0.6 was used (see trees in Fig. 6). The two hedge-types were modeled as 1 m tall, one as conifer, one as deciduous and the height of the grass was set to 0.1 m.

Several construction phases during the long history of the campus resulted in several different building typologies (see Fig. 5). Table 3 shows the four building categories that were used to group the buildings according to their construction type and the specifications of wall and roof construction. In Table 4, the physical properties of the used materials are listed. The most common building type on campus is that of category D (11 buildings), followed by C (4 buildings), B (3 buildings) and A (1 building). Dating back to a time before the foundation of a university in Gløshaugen, the wooden buildings are rather small and not typical institutional buildings, so that wood is the least used façade material on campus. In all the other buildings, the building facades are characterized by heavy materials.

3.2. Validation

Validation is the process of determining how well the computerized model within its domain of applicability represents the real world with a satisfactory range of accuracy, by using physical observations. In other words, it makes sure that a numerical model within a certain range of acceptability is accurate enough for its intended use [77,78]. In practice, the quality of the results not only depends on the accuracy of the model itself but to a considerable degree also on the input provided by the users [91]. Consequently, the user's decisions regarding simplifications and experience in using the software can lead to substantial discrepancies, as found for instance in the case of building performance simulation (BPS) by Imam et al. [92].

The numerical model that was used in this study was created following the design-framework in Fig. 8. The model input for the meteorological boundary conditions was supplied by using the *intermediate* and *full forcing* option in ENVI-met.

The *full forcing* option facilitates variable meteorological boundary conditions (30-min intervals) for air temperature, relative humidity, solar radiation, as well as wind speed and direction. These input boundary conditions were generated from the measured meteorological data retrieved from the reference weather station on the VATL building. To split the measured global horizontal radiation into its direct and diffuse components as required for the input file in ENVI-met, the model by Skartveit and Olseth [93] was applied. Specifically developed for average snow-free conditions close to sea level in Norway, it was assumed to represent a suitable approximation.

The validation process consisted of three stages in which a different number of nesting grids were used, and adjustments of the meteorological boundary conditions were made in order to fit the measurements of the fixed and the four mobile weather stations as well as the IR thermography. An overview of the different calibration stages and their average R^2 and coefficient of variation of the root mean square error, the CV(RMSD), can be seen in Table 5. The equation for determining the CV(RMSD) can be seen in Eq. 1, where s_i and m_i are the simulated and measured value of time step i, respectively, n is the total number of time steps and $\bar{m}$ is the mean value of measurements.

Table 2
Measurement equipment used in the mobile weather stations.

Type of measurement	Measurand	Sensor	Accuracy
In-situ measurements	Wind direction	S-WDA-M003	±5° at 1.4° resolution
	Wind speed	S-WSB-M003	±1.1 m/s or ±4% of reading
	Air temperature	S-THB-M002	±0.21 °C from 0 °C to 50 °C
	RH of air	S-THB-M002	±2.5% from 10% to 90%
IR thermography	Surface temperature	AC080V	±2 °C or ±2% from –20 °C to +350 °C

Fig. 7. 3D bird's eye view of the numerical model. Perspective from the northwest (NW).

Table 3
Building categories according to construction type and specifications of walls and roofs.

Category	Year of construction	Type	Layer 1 (outside)		Layer 2		Layer 3 (inside)	
			Material	d [m]	Material	d [m]	Material	d [m]
A	1850–1900	Wall	Wood: spruce	0.06	Insulation	0.08	Wood: spruce	0.06
		Roof	Roofing: tiles	0.03	Wood	0.04	Insulation	0.2
B	1910	Wall	Granite	0.3	–	–	–	–
		Roof	Roofing: tiles	0.03	Wood	0.04	Insulation	0.2
C	1910–1924	Wall	Solid brick	0.3	–	–	–	–
		Roof	Roofing: tiles	0.03	Wood	0.04	Insulation	0.2
D	1951–2002	Wall	Filled concrete blocks	0.3	–	–	–	–
		Roof	Bitumen	0.02	Insulation	0.2	Concrete	0.3

Table 4
Selected physical properties of the building surface materials on campus [88–90].

Surface	α [–]	ω [–]	ε [–]	c [kJ/(kgK)]	δ [kg/m^3]	λ [W/(mK)]
Wood: spruce	0.6	0.4	0.9	1600.0	450.0	0.12
Concrete	0.7	0.3	0.9	840.0	1260.0	0.85
Insulation	–	–	–	1030.0	50.0	0.045
Granite	0.8	0.2	0.9	1000.0	2600.0	2.8
Bitumen	0.92	0.08	0.9	1000.0	1050.0	0.17
Solid brick	0.6	0.4	0.9	1000.0	2400	1.4
Glass: clear float	0.05	0.05	0.9	750.0	2500.0	1.05

Absorptivity (α), reflectivity (ω), emissivity (ε), heat capacity (c), density (δ), thermal conductivity (λ)

A previous investigation of different grid spacing showed disproportionally long simulation times for finer grids than the used one. The discretization in a 4 × 4 × 3 m^3, therefore, represents the finest, computationally still acceptable grid. Coarser grids were omitted as they are not able to sufficiently catch the geometrical features of the study area. The initial ENVI-Met model constitutes stage 1. In stages 2 and 3, the inlet air temperature $T_{a,in}$ and the inlet wind speed $u_{w,in}$ from the forcing file were reduced by 0.5 °C and 25%, respectively. Also, the number of nesting grids was increased from 0 in the initial model to 6 in stage 2, and 15 in stage 3.

$$CV(RMSD) = \frac{RMSD}{\bar{m}} \times 100\% = \frac{\sqrt{\sum_{i=1}^{n}(s_i - m_i)/n}}{\bar{m}} \times 100\,\% \qquad (1)$$

As can be seen from the calibration results, increasing the number of nesting grids did only marginally affect the accordance of simulated meteorological values with the measured ones. Fig. 9

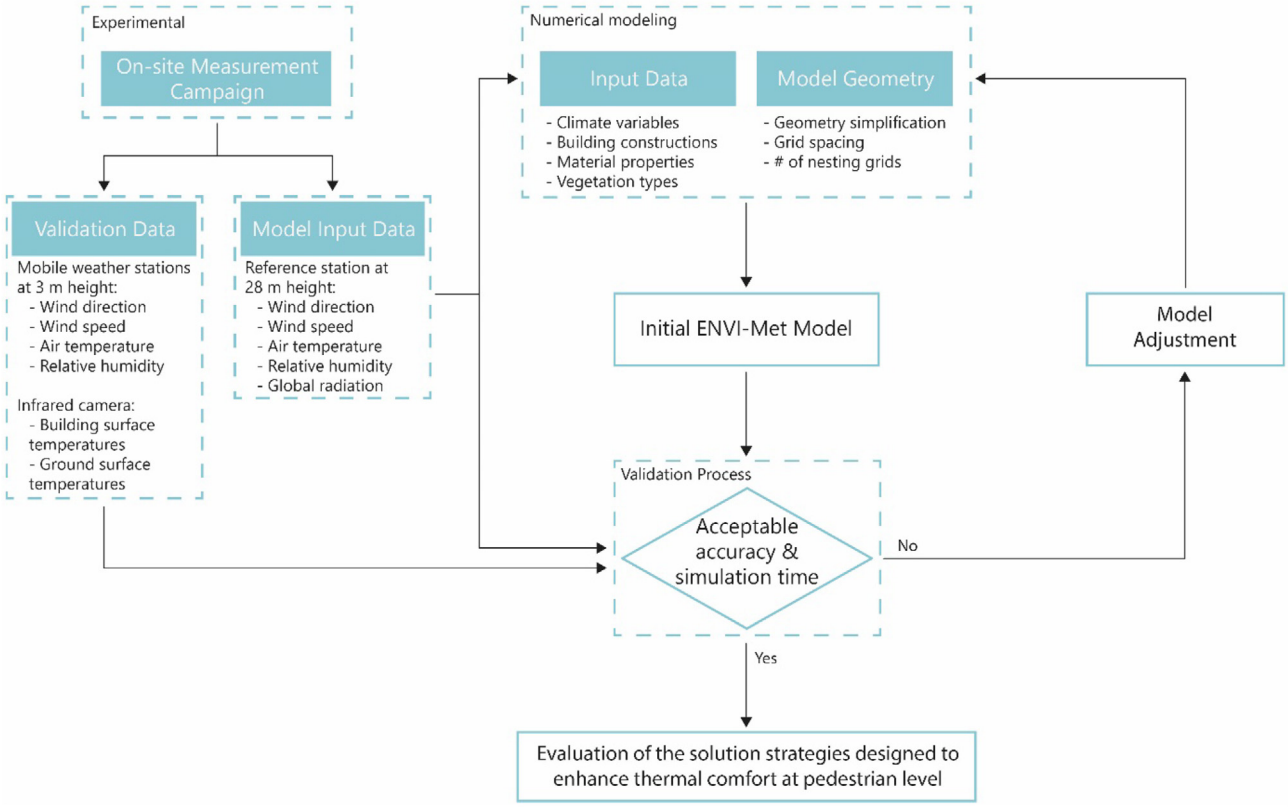

Fig. 8. Applied design framework for creating the ENVI-Met model, modified from [80].

Table 5
Overview of calibration stages and quality measures to compare simulated and measured data.

	Number of nesting grids	Adjustments of meteorological conditions	Mean R^2 of climate variables	Mean CV (RMSD) of climate variables	Mean absolute difference of surface temperatures
Stage 1 (initial model)	0	–	0.55	101.2%	4.58 °C
Stage 2 (selected)	6	$T_{a,in}$ reduced by 0.5 °C $u_{w,in}$ reduced by 25%	0.56	75.4%	2.86 °C
Stage 3	15	$T_{a,in}$ reduced by 0.5 °C $u_{w,in}$ reduced by 25%	0.54	76.5%	4.02 °C

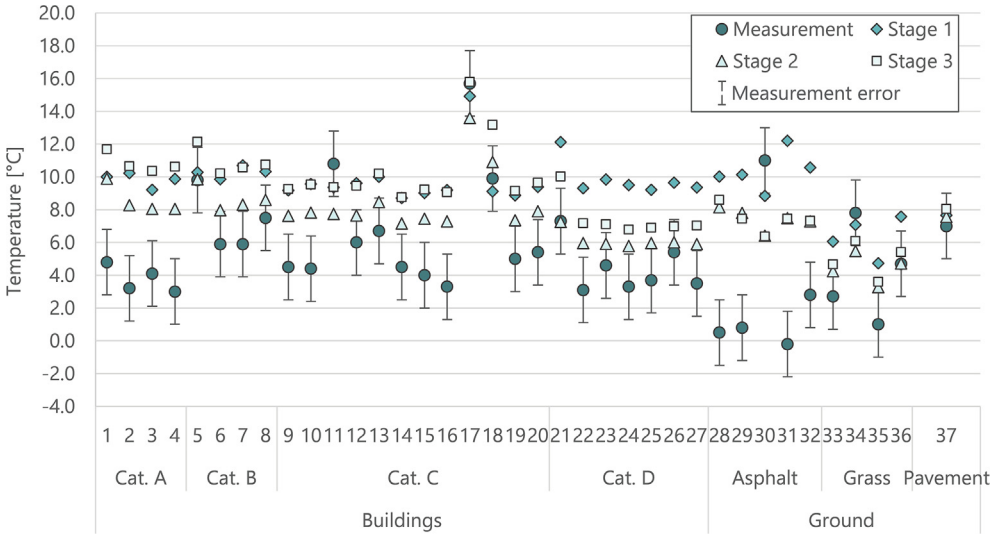

Fig. 9. Measured and simulated surface temperatures of the calibration stages at the 37 measurement spots. The bars above and below the measurement values indicate the measurement errors associated with the accuracy of the IR camera.

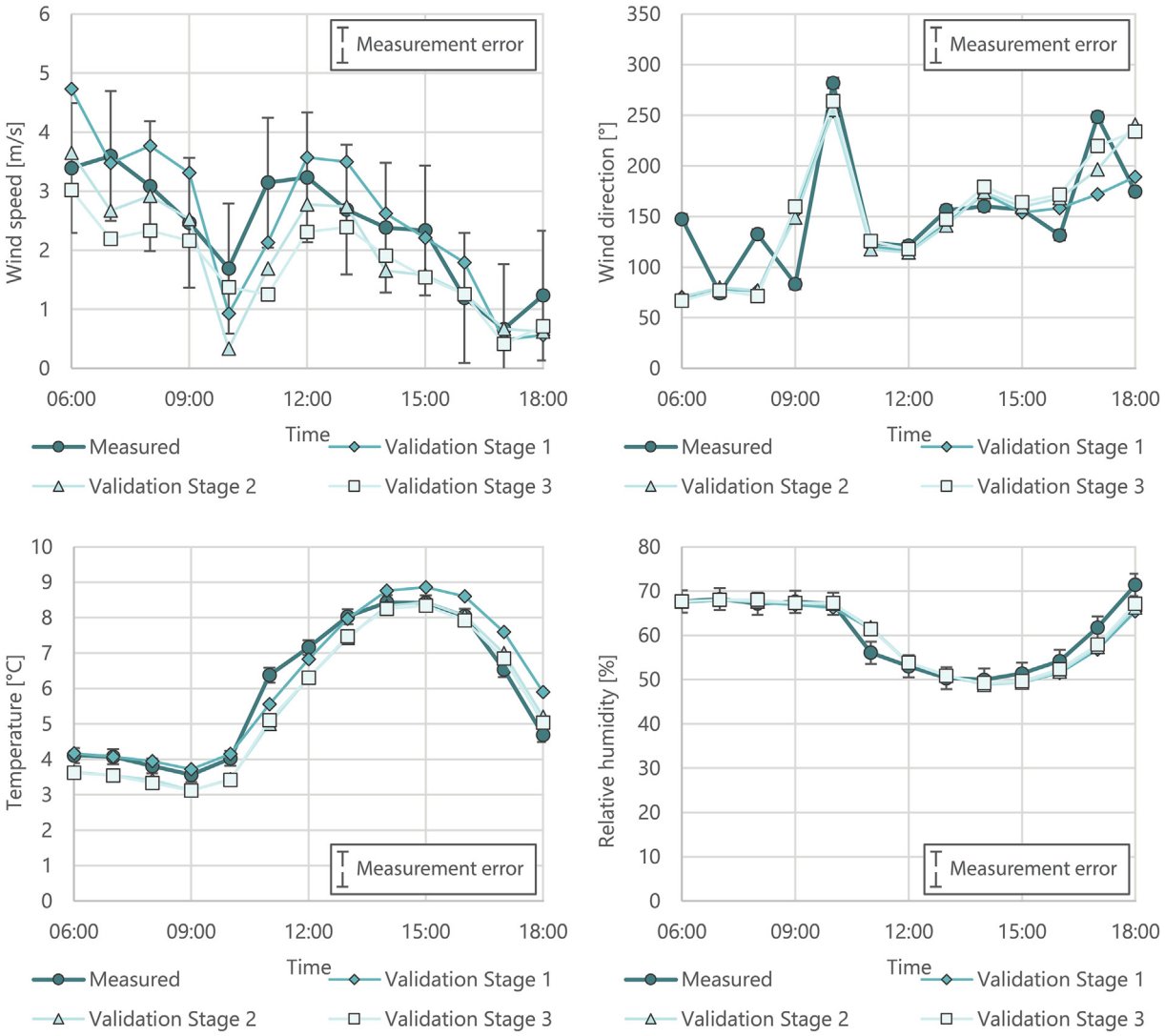

Fig. 10. Measured and simulated climate variables of the calibration stages at the VATL reference weather station. The bars above and below the measurement values indicate the measurement errors associated with the accuracy of the sensors.

and Fig. 10 show the measured and simulated climate variables including the measurement error resulting from the sensor accuracy. On the contrary, the mean absolute difference of simulated and measured surface temperatures was subject to a noticeable variation. The simulations largely overestimate the measured surface temperatures. Especially in building category A and the ground surfaces of type *asphalt*, the simulation results significantly surpass the measurements.

In Fig. 10, the measured and simulated climate variables at the reference weather station on the VATL building are plotted. As visible from the graphs, the course of the measured values is followed by the simulations to a large extent. The validation assessment shows overall good results (see Table 6). Especially stage 2 shows a good correlation (average $R^2 = 0.85$) on modeled air temperature, a moderate correlation (average $R^2 = 0.40$) on modeled wind speed and a good correlation (average $R^2 = 0.80$) on modeled relative humidity. The CV(RMSD) of modeled air temperature and relative humidity in this stage was 9.3% and 7.7%, respectively. The model of stage 2 was considered valid for the set of experimental conditions, as its accuracy is within an acceptable range. Therefore, the model of stage 2 was used in the simulations for the analysis of this study.

However, the model results do not provide adequate accuracy on wind direction data. This may be caused by placing the weather stations close to buildings where turbulence is usually very high. Using a wind vane to capture the direction of the flow will inevitably lead to high uncertainty of the measurement compared to an undisturbed, open setting. Furthermore, it can be noticed that the CV(RMSD) of the wind speed and wind direction in particular are very high. This can be partly explained, as the used measurement equipment to capture wind speed and direction has a relatively high sensitivity threshold of 1 m/s. The measured wind speeds were, therefore, often 0 m/s, while in the simulations, also wind speeds below this threshold occurred. As there are many 0-measuements, calculating the CV(RMSD) of these climate variables results in very high values. Analogously, at wind speeds below 1 m/s, the wind vane of the wind direction sensor will not move to the respective wind direction, while in ENVI-Met such a sensitivity threshold does not exist and every air movement, no matter how small, is captured with its velocity and direction.

3.3. Design strategies for improving urban microclimate and outdoor thermal comfort

As shown in chapter 2, summers in Trondheim are relatively short and mild. With an average monthly temperature of about 12–15 °C and generally less windy conditions, the summer months

Table 6
R^2 and CV(RSMD) of all the validation data. The values with the best accordance with the measurements of each category are highlighted in bold.

Weather station	Climate variable	Stage 1		Stage 2		Stage 3	
		R^2	CV (RMSD)	R^2	CV (RMSD)	R^2	CV (RMSD)
VATL	Wind speed	0.85	**27.6%**	0.74	31.2%	**0.92**	37.2%
	Wind direction	0.02	**27.0%**	**0.05**	27.6%	**0.05**	27.5%
	Air temperature	**0.93**	**9.2%**	0.91	10.2%	0.89	9.7%
	Relative humidity	**0.91**	4.5%	**0.91**	4.2%	0.88	**3.7%**
Station A	Wind speed	0.42	172.3%	0.36	95.9%	**0.45**	**63.8%**
	Wind direction	0.01	**40.1%**	**0.16**	109.9%	0.00	102.1%
	Air temperature	**0.85**	15.0%	0.81	**9.5%**	0.83	10.0%
	Relative humidity	**0.78**	10.2%	0.73	9.2%	0.76	**9.1%**
Station B	Wind speed	**0.38**	1018.3%	**0.38**	**672.1%**	**0.38**	713.0%
	Wind direction	0.15	**74.9%**	**0.22**	79.3%	0.13	75.0%
	Air temperature	**0.82**	16.6%	**0.82**	10.2%	0.79	**8.8%**
	Relative humidity	**0.76**	10.9%	**0.76**	**9.8%**	0.73	**9.8%**
Station C	Wind speed	0.39	250.6%	0.39	**160.9%**	**0.40**	166.6%
	Wind direction	0.27	**41.9%**	**0.40**	52.6%	0.27	58.3%
	Air temperature	**0.86**	11.2%	**0.86**	8.1%	0.81	**6.4%**
	Relative humidity	**0.80**	8.1%	**0.80**	**6.7%**	0.75	**6.7%**
Station D	Wind speed	0.16	218.7%	0.18	**158.2%**	**0.29**	160.0%
	Wind direction	0.00	44.5%	0.00	**35.8%**	0.00	47.3%
	Air temperature	**0.88**	12.0%	0.87	8.8%	0.82	**7.8%**
	Relative humidity	**0.80**	9.6%	0.79	8.3%	0.70	**8.1%**
Average		0.55	101.2%	**0.56**	**75.4%**	0.54	76.5%

from June to August, in general, provide good conditions for spending time outdoors, apart from the many showers of rain that frequently occur throughout the year in the area [75]. Regarding OTC research in this kind of climate, the focus should be put on winter and the transitional seasons rather than summer. Thus, the aim of this study is to promote outdoor activities and extend the period in which people feel comfortable being outside at the university campus during the transitional season of autumn.

The weather conditions of the day that was used for the validation (October 20th, 2019) can be regarded as a typical, sunny autumn day, as its mean temperature (5.5 °C) and wind speed (2.22 m/s) were in close vicinity to the average values for Trondheim for the period from September to November (6.3 °C and 2.45 m/s for the years 2009–2018). Hence, the following solution strategies were simulated using the same weather conditions as for the validation except for the wind direction. Since there were strong fluctuations in wind direction on the validation day, the prevailing wind direction for Trondheim during autumn, which is 225° from North (SW), was used. SW is the prevailing wind direction throughout the whole year.

The frequently used Predicted Mean Vote for outdoor conditions (PMVo), originally developed by Fanger [94] for indoor conditions (PMV) and adapted for outdoor by Jendritzky and Nübler [95], served as an indicator of OTC in this study. The software ENVI-Met applies the PMVo equations on a 9-point scale (−4 very cold, −3 cold, −2 cool, −1 slightly cool, 0 neutral, 1 slightly warm, 2 warm, 3 hot, 4 very hot) as described in the German VDI 3787 Part 2 [96]. Although originally developed for the application indoors, the PMV was chosen as it represents the most renowned comfort index and is expected to deliver meaningful results as it has been adapted to the use for outdoor spaces. The PMVo has been applied in many other studies of OTC using ENVI-met and can therefore be considered as a reliable indicator for this study's purpose [26,68,69,97].

As outlined in the introduction, people in cool or wintry conditions prefer higher air temperatures and solar radiation, as well as lower wind speeds. These variables are key parameters in evaluating thermal comfort in a comfort index like the PMVo. Hence, solution strategies in the built environment need to take them into consideration in order to improve OTC. The recognized measures to counteract overheating in cities and tackle people's heat stress in regions with hot summers provide useful guidance for this study's purpose, as the exact opposite is supposed to lead to suitable solutions. Thus, decreasing the surface albedo to increase solar absorption and thus surface temperatures and the emittance of longwave radiation may have a favorable effect on OTC. Additionally, the decrease of the wind speed through vegetation or constructive elements like buildings or walls, wind shelter, etc. may locally improve OTC conditions. Finally, increasing solar access in frequently-occupied spaces, for example by removing redundant vegetation, etc. may have a beneficial impact.

With this in mind, four scenarios have been developed and investigated (see Fig. 11) to improve OTC at 12:00 local time in the most-occupied outdoor space on campus, "Stripa" (see Fig. 3 and Fig. 4). 12:00 was selected because people use to spend their lunch break outside near the Café on sunny days or change buildings for lectures, using Stripa as the main connection.

The scenarios build upon the current situation which represents the base case of this study (see Fig. 7). In its current form, greenery covers about 48% of the area at ground surface level (3% trees and hedges, 45% grass). The remaining area is covered by buildings (26%), asphalt (16%), and pavement (10%). The surface materials of the buildings are defined by their building category and their respective wall constructions which can be seen in Fig. 4, Table 3 and Table 4.

In scenario a) all the trees have been removed from the study area. The next two scenarios aim to reduce the wind speed by "closing" the entrances in the East, West and South of the campus with building structures (b) and trees (c). In scenario b), the inserted buildings were modelled to be of the same height as the structures on each side of the passages that they close. In the case of the two passages in the east, the inserted buildings were 12 m, in the two southern passages they were 14 m, and in the western passage, the building was 16 m high. In scenario c), the passages were closed with one row of 20 m high trees (Norway Maple). Scenario d) addresses the building surfaces by adding a dark façade cladding in the form of charred wood panels to the base case. The darker color at the surfaces generally leads to higher surface temperatures and thus a higher mean radiant temperature (MRT).

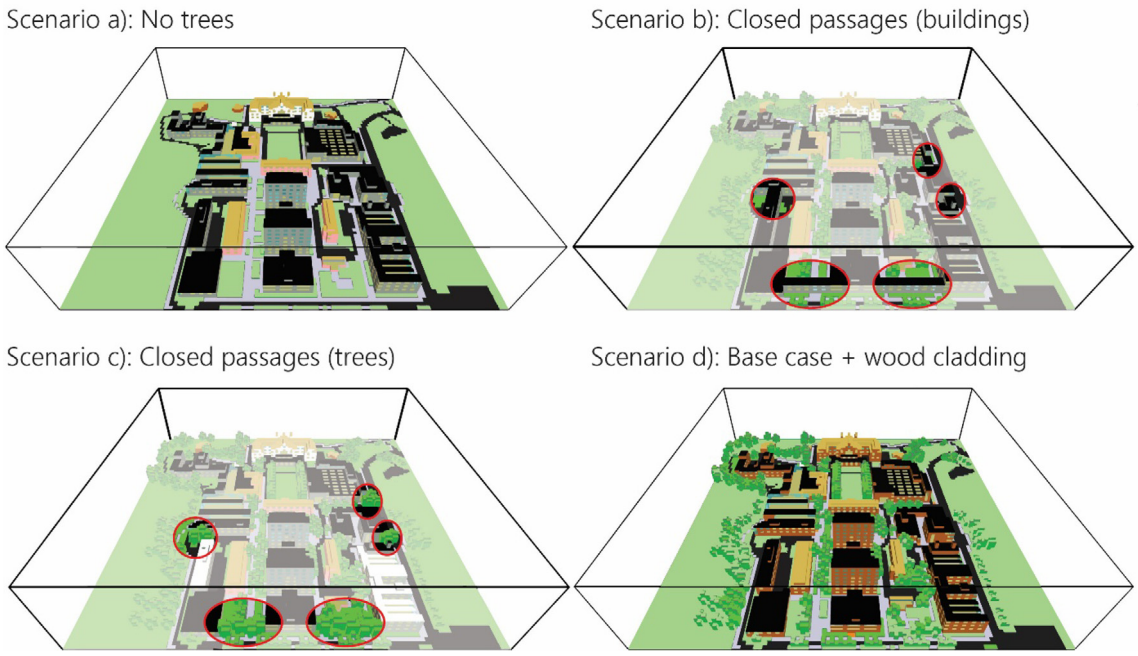

Fig. 11. Bird's eye views of scenarios a) to d).

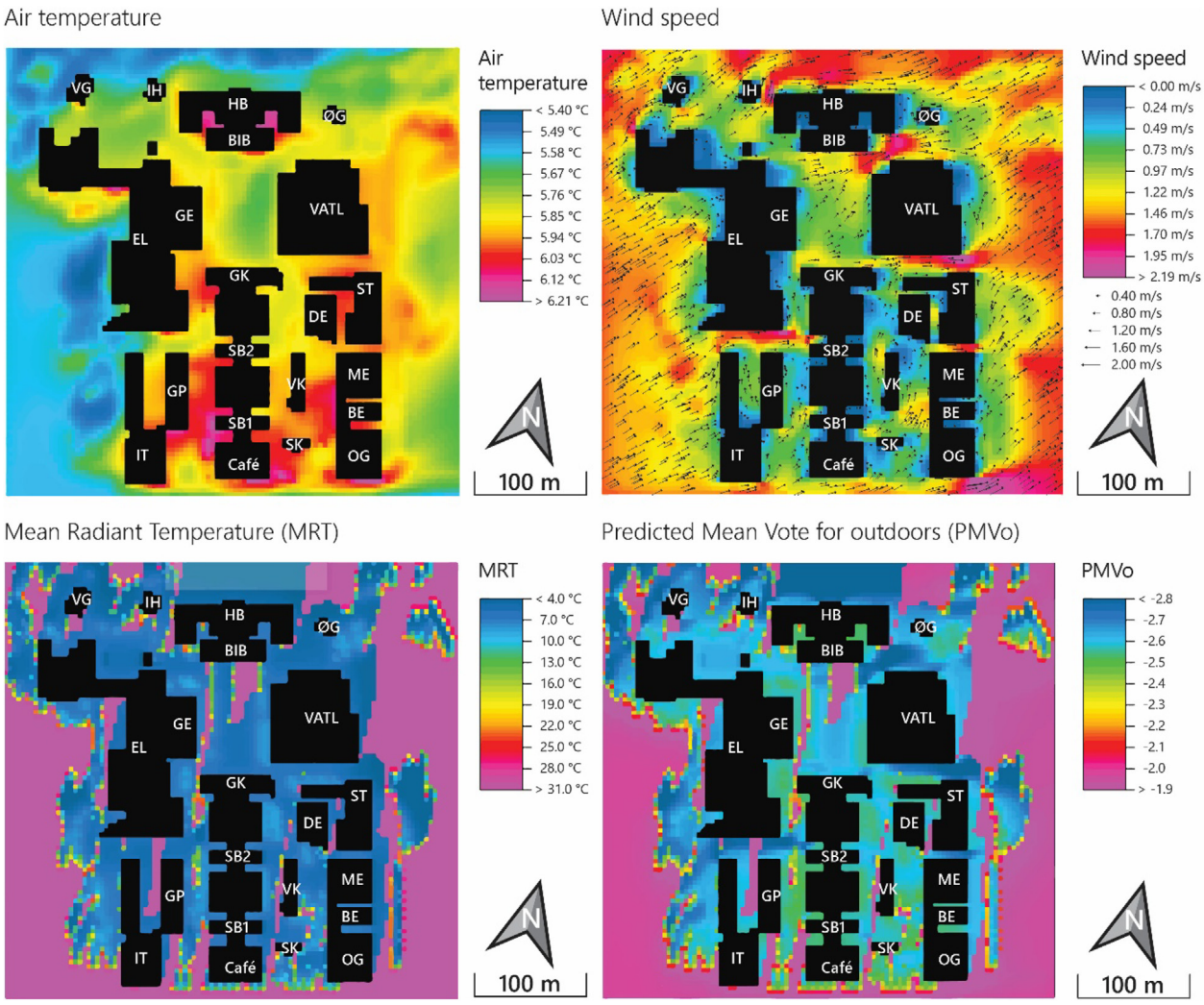

Fig. 12. The simulated spatial distribution of the air temperature, wind speed, MRT and PMVo for the campus in its current situation (base case).

4. Results

4.1. Base case

Fig. 12 shows the air temperature, the wind speed, the MRT, and PMVo of the campus in its current situation (base case). The PMVo was calculated at the pedestrian level (1.5 m) for an average 22-year-old person (male) with 75 kg, a metabolic rate of 1.52 met (activity: walking at 1.2 m/s) and a clothing level of 1.2 clo (regarded as typical for autumn). The spatial data visualization was performed with LEONARDO, ENVI-met's module for visualizing and analyzing the performance of the model environment.

The PMVo values for a typical day in October in the study area were between −2.8 (cold) and −1.9 (cool), with the highest values occurring in areas where unobstructed solar radiation is available. The lowest values were reached in shaded areas where additionally high wind speeds occur which was mostly the case in narrow passages between buildings. There, channeling effects accelerated the air from the inlet wind speed of 2.2 m/s to a top speed of up to 2.5 m/s. At Stripa, the average values for air temperature, wind speed, MRT and PMVo were calculated as 6.54 °C, 0.78 m/s, 12.45 °C and −2.72 respectively.

4.2. Strategy evaluation

The simulated results (for a typical autumn day at 12:00) show that the suggested strategies have a small effect on OTC. The examined solutions aimed at improving the thermal sensation of the humans and thus increasing the PMVo (through addressing different microclimatic parameters such as the solar radiation, the air temperature, the MRT and the wind speed). The simulated scenarios indicate that significant improvements in terms of the PMVo (up to 1.1 higher) at the pedestrian level were only possible if the solar access was maximized (see Fig. 13).

4.2.1. Air temperature

In scenario a), where all trees were removed from the study area, the largest improvement of air temperature at Stripa was registered with 0.37 K in front of the EL building (see Fig. 13). Where trees in the base case obstructed the sun, it now warms up the ground and building surfaces, causing the air temperature close-by to rise.

In scenario b), changes in air temperature of this magnitude only occurred directly in front of the south façade of the inserted building west of the Café at Stripa's southern entrance. There, unobstructed solar radiation reaches the south-facing building surface all the way down to the pedestrian level and thus causes air temperatures to rise. However, at Stripa, shadowing from buildings and trees largely prohibit positive changes in air temperature at the pedestrian level, as the obstructed sun cannot warm up the building surfaces close to the ground. For that reason, the air temperature at the pedestrian level remains close to unchanged in scenario d). On the contrary, the newly inserted building in scenario b) which is meant to provide protection from wind, obstructs incoming solar radiation and therefore causes the air temperature to decrease by up to 0.31 K near the SB1 building and the Café. The same is visible in scenario c) where additional trees at Stripa's southern entrance cast more shadow and thus prevent surfaces nearby to warm up. On average, however, the change in air temperature was negligible in all the investigated scenarios (see Fig. 17).

4.2.2. Wind speed

Removing the trees in scenario a) had an amplifying effect on wind speed as visible from Fig. 14. Almost throughout the entire extent of Stripa, the wind speed increased with reaching values up to 26.3% higher than in the base case. Only in the wake of the GP building at the northern end of the examined area, wind speed slightly decreased by up to 9.4%. On average, values increased by 10.7% in scenario a). Conversely, inserting buildings to close the southern and western entrances to Stripa contributed to a lower wind speed in scenario b) where the average values went down by 3.7%. Maximum reductions reached 46%. In scenario c), adding more trees to the entrance areas in the West and South resulted in only 0.6% lower average values where the largest decrements reached 13.7%. In the scenarios b) and c), significant increases in wind speed occurred only in the very south of Stripa with 14.1% and 10.3%, respectively. Naturally, the change of the surface materials as in scenario d) did not have a noteworthy impact on the

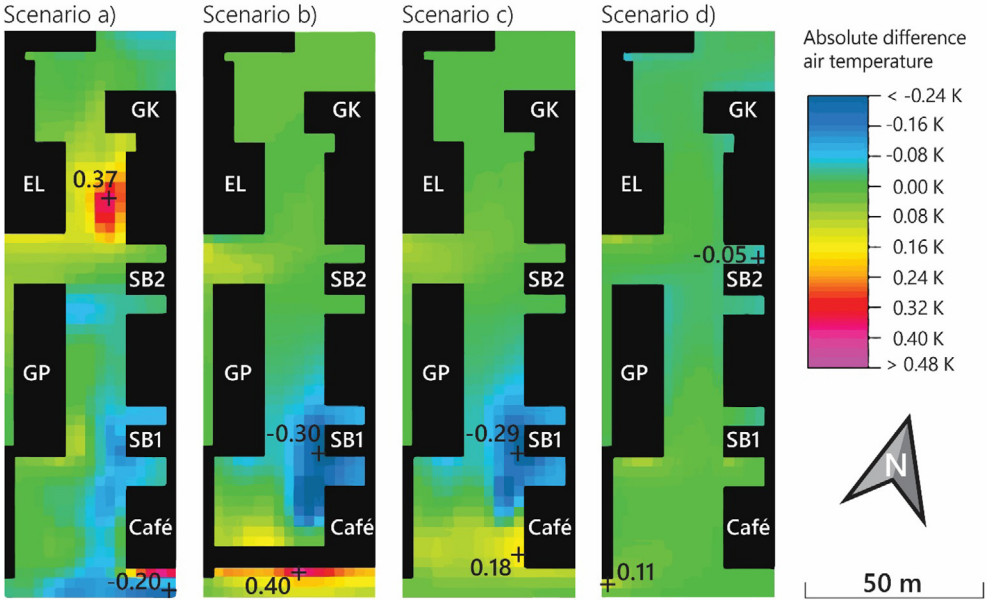

Fig. 13. Absolute change in air temperature in the examined area Stripa at 12:00 at pedestrian level (1.5 m) of the scenarios a) to d) compared to the base case. The crosses indicate the spots with the highest and lowest value of each scenario.

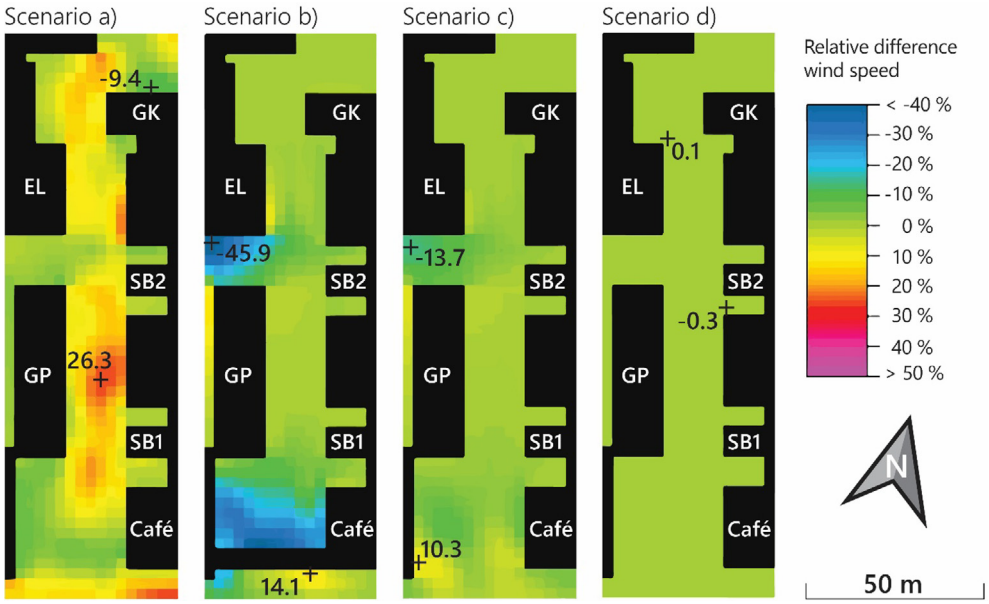

Fig. 14. Relative difference of wind speed at Stripa at 12:00 at pedestrian level (1.5 m) of the scenarios a) to d) compared to the base case. The crosses indicate the spots with the highest and lowest value of each scenario.

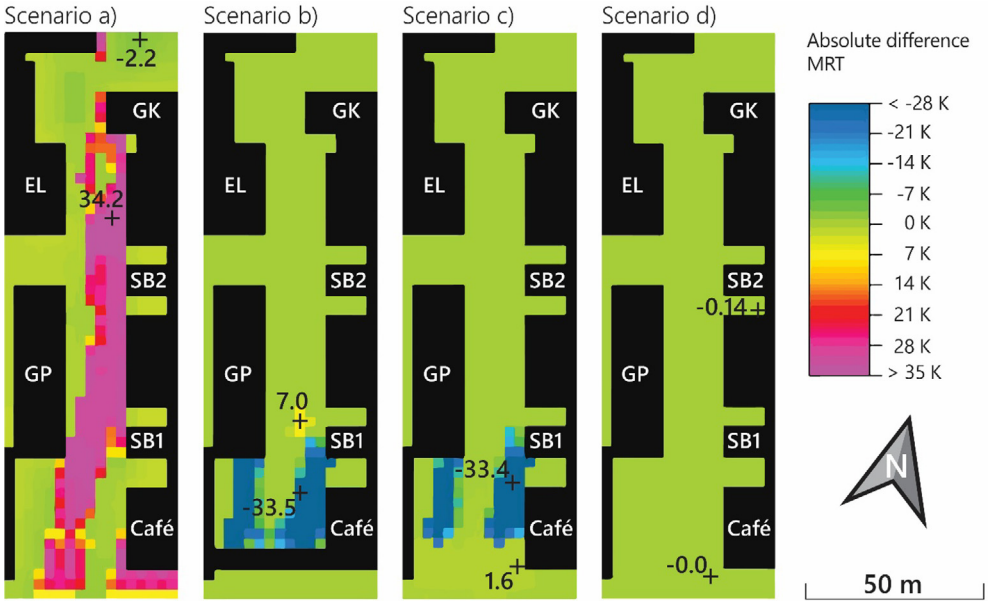

Fig. 15. Absolute change of MRT at Stripa at 12:00 at pedestrian level (1.5 m) of the scenarios a) to d) compared to the base case. The crosses indicate the spots with the highest and lowest value of each scenario.

wind field. The average value at Stripa for the wind speed remained unchanged.

4.2.3. Mean radiant temperature and PMVo

Fig. 15 and Fig. 16 show the change of MRT and PMVo for the scenarios a) to d) compared to the base case. The visual similarity of both parameters' colormaps illustrates the strong correlation between the MRT and PMVo. Consequently, in areas of an increased MRT compared to the base case, also the PMVo values were improved. Especially in scenario a), where removing the trees resulted in maximized solar access, the change in MRT and PMVo reached top values of 34.2 K and 0.95, respectively. There, the points in which the maximum and minimum values almost match. In scenario b, the average MRT and PMVo at Stripa improved by 13.9 K and 0.33, respectively.

Similarly, in scenarios b) and c) the largest decreases of MRT and PMVo roughly coincide in the same points. This is because the added building and trees in the south of Stripa obstruct the sun, causing the MRT and the PMVo to drop by up to 33.5 K or 0.80, respectively. While in the scenario b), the average MRT, compared to the base case, slightly improved by 0.02 K, the PMVo dropped by 0.08 at Stripa.

In scenario c), the effect of additional trees resulted in both, a lower average MRT (−0.11 K) and PMVo (−0.06) compared to the base case at Stripa. In scenario d) however, where a lower surface albedo was expected to result in higher surface temperatures and

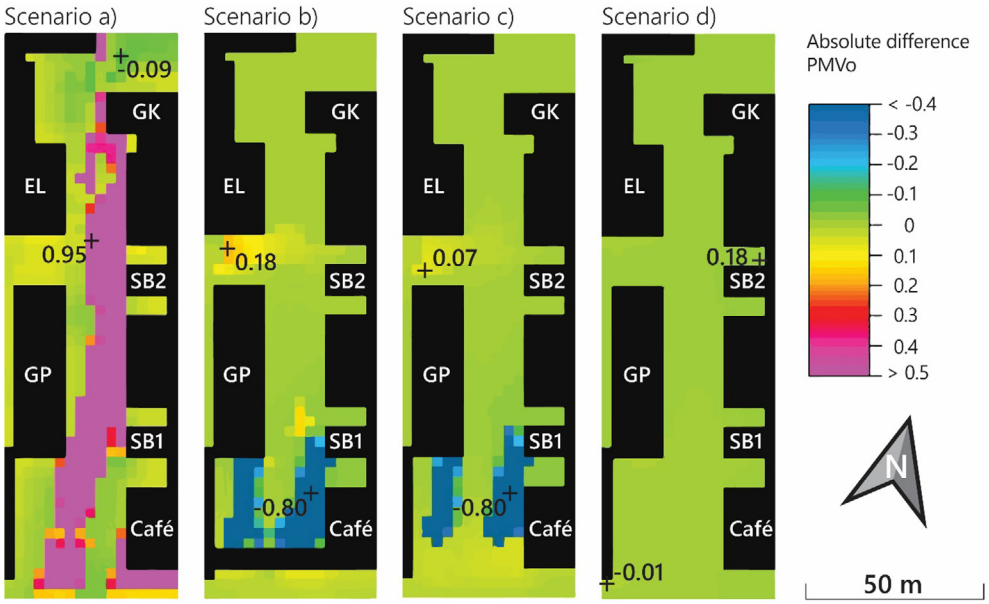

Fig. 16. Absolute change of PMVo at Stripa at 12:00 at pedestrian level (1.5 m) of the scenarios a) to d) compared to the base case. The crosses indicate the spots with the highest and lowest value of each scenario.

thus higher MRT and PMVo, the exact opposite effect was identified. The average MRT and PMVo both slightly decreased at Stripa. This is because, during the cold season in a high-latitude location as Trondheim, only little solar radiation reaches building surfaces at the pedestrian level due to low solar angles. Shadowing from buildings and trees in this scenario does not allow to make use of the new façade properties. Consequently, a different surface material will generally have a rather small effect on the MRT and hence the PMVo. The largest improvements in PMVo in the scenarios b) and c) are attributable to reduced wind speed near the closed western entrance to Stripa. There, maximum improvements were 0.18, 0.07 and 0.18, respectively. Again, in scenario d), changes were negligible.

5. Discussion

In summary, most pronounced improvements were achieved with maximizing solar access. The difference between shaded and unshaded areas with otherwise equal conditions on the simulated day can be quantified with a PMVo of ca. 1.0. Having in mind the variability in meteorological conditions, particularly in solar radiation, wind sheltering can be an effective measure to increase OTC, especially on windy days. This is particularly the case when days get even shorter and sun angles lower in winter. The effect of wind-sheltering, however, was found to be quite local. Considerable reductions of the wind speed occurred only within a range of 1.0–2.5 times the height of the inserted buildings and 0–1.5 times the height of the inserted trees. However, only one row of 20 m high Norway Maple trees was placed in the passages. Inserting a mix of small and high conifers in addition in two or more rows might reduce the wind speed more effectively [98]. Additionally, the sheltering elements may provide additional shade which leads to an overall negative effect on sunny days when sun angles are not too low.

On the simulated, typical and sunny autumn day in Trondheim with a comparatively low wind speed of 2.2 m/s as an inlet condition, access to solar radiation turned out to be significantly more effective than wind protection. The former was able to increase local PMVo values by up to 1.0 compared to shaded areas while the latter accounted for improvements not exceeding 0.6 on the campus. At Stripa on the other hand, the effects of increased solar access and wind sheltering were lower, as it improved local PMVo values by 0.95 and 0.18 respectively. These results corroborate the findings from other studies that solar radiation is one of the most important factors for OTC and that it is more important than wind sheltering [60,61,63,64].

As the resulting changes in PMVo are comparatively small, wind sheltering in locations with rather low average wind speeds cannot be regarded as a suitable strategy to improve outdoor thermal comfort on a larger scale. This especially applies to areas, where people tend to move around such as pedestrian zones. In areas, however, where people tend to stay in one area, like seating areas in cafés for instance, wind sheltering can be used to improve outdoor thermal comfort. More customized design solutions than the ones investigated in this study are necessary in order to achieve larger improvements of OTC. Similar design considerations were given by Leng et al. [99] who stress the consideration of solar access in the design of public spaces, as people in winter cities, during the transional seasons, tend to seek sunlight. They also refer to sheltered sitting areas and heated seats.

Simulations with a higher wind speed showed that wind sheltering can become more effective in increasing the PMVo than solar access. From about 8 m/s imposed at the inlet, both measures became equally effective in increasing OTC. As a solution, transparent wind sheltering elements e.g. around outdoor sitting areas (for instance from glass) may be able to provide near unobstructed solar access and protection from the wind at the same time. Introducing darker surface materials to building façades in order to increase the MRT had a negligible effect on the microclimate and thus OTC, as low solar angles during the cold seasons prevent solar radiation to warm up the surfaces. As Jamei et al. [100] concluded in their review on the impact of urban geometry and pedestrian level greening on OTC, a larger distance between buildings is necessary in high-latitude locations to avoid overshadowing and thus increase solar access. It can be seen in Fig. 7 and Fig. 11 that Stripa is shaded during the morning hours by numerous trees and the two large buildings (SB1 and SB2) in the east. At lunch time, the sun reaches a sufficient elevation and azimuth to finally reach pedestrian level surfaces. However, without solar access over a

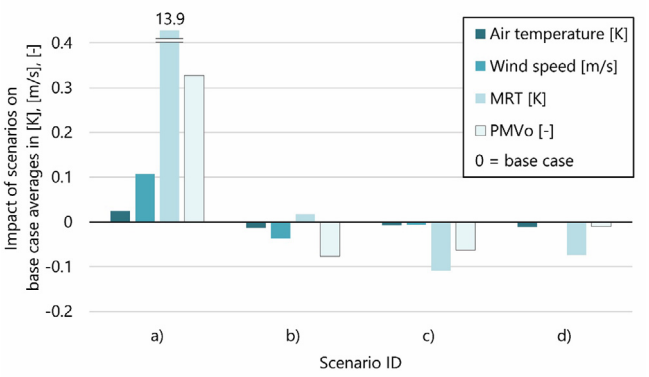

Fig. 17. Impact of the investigated microclimatic design scenarios a) through d) on average air temperature, wind speed, MRT and PMVo when compared to the base case at Stripa.

sufficient time span, changing the surface materials consequently has a negligible influence on OTC at the investigated location and time. Fig. 17 sums up the changes in the investigated scenarios at Stripa and shows the direction and magnitude of change of the different variables of the four scenarios compared to the base case averages. Fig. 18 visualizes the resulting predicted percentage of dissatisfied (PPD) for all investigated scenarios as well as the base case. Only scenario a) noticeably improved the situation, while the scenarios b) and c) affected the OTC slightly negative at Stripa. Scenario d) resulted only in marginal changes.

With regard to the software ENVI-Met which was used to create the numerical model, some limitations apply in this study as well. First of all, ENVI-Met does not allow to depart from a fixed, structured grid when setting up the geometry of the model area. Curved and sloped surfaces need to be approximated with square blocks, which not only influences their orientation and aerodynamics but also increases the surface area of these elements. For this study, a 4-m grid was chosen to ensure acceptable simulation times and accuracy, as it was not possible refining the grid in the areas of interest while coarsening it at the boundaries. Furthermore, the program's output is time- (hourly) and space-averaged (per grid cell). Especially in the validation of the model these limitations might explain part of the deviations between measurements and simulations. However, the investigated climate variables were represented reasonably well by the numerical model.

6. Conclusion

In this study, numerical simulations of the urban microclimate of a university campus in Trondheim, Norway were carried out with ENVI-met. The numerical model was validated with on-site measurements of wind speed, wind direction, air temperature, humidity, and surface temperatures taken in autumn 2019. The validated model was used to investigate four scenarios: (a) removing all trees from the study area, (b) closing the passages with buildings and (c) trees, and (d) changing the surface material of the buildings.

When designing public spaces in a cold climate like in Norway, the access to solar radiation proved to be a key element to provide OTC. Wind sheltering also enhanced OTC conditions, although not quite as sharply outlined as solar access. However, on particularly windy and cloudy days, wind sheltering is the only effective way to increase OTC. Thus, a combination of both, increased access to solar

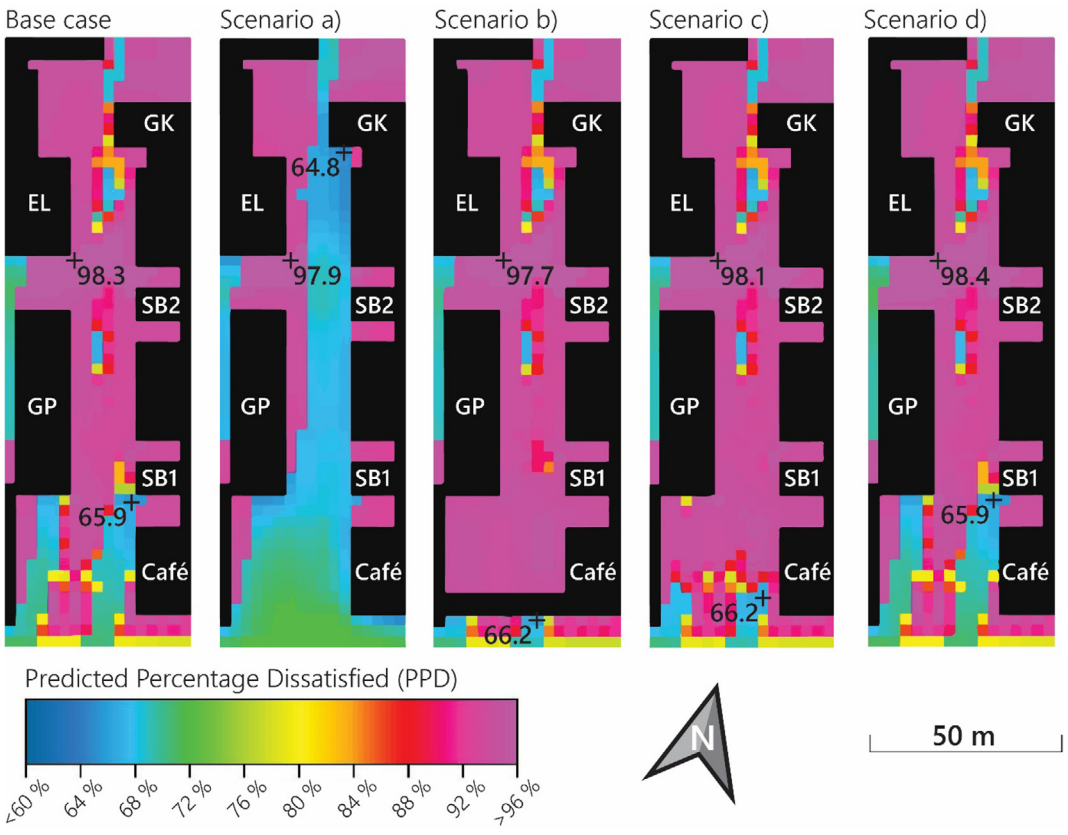

Fig. 18. PPD at Stripa at 12:00 at pedestrian level (1.5 m) of the base case and scenarios a) to d). The crosses indicate the spots with the highest and lowest value of each scenario.

radiation and protection from elevated wind speed can effectively increase OTC and consequently promote outdoor activities and make people stay outdoors longer. Increasing the albedo of the building surface materials had an insignificant effect on OTC as the solar angles during the cool and cold seasons in a city with typical building-height-to-street-width ratio at this latitude are too low to significantly increase surface temperatures and thus the MRT and PMVo at pedestrian level.

This study has gone some way towards enhancing our understanding of the design of open spaces in high-latitude urban settlements. We have obtained comprehensive results showing the effect of solar access and wind sheltering to enable thermal comfortable environments in outdoor areas. Furthermore, this study has shown that reversing design interventions which proved to be effective and are typically used in warmer climates to mitigate the UHI like changing the albedo of surface materials, are not as effective in high-latitude locations due to less solar incidence and lower sun angles during the cold season.

This study helped to understand the effect of different interventions with the urban environment on OTC. It confirms that of the microclimatic parameters that affect people's comfort only solar radiation and wind can be favorably modified by the surrounding. Further research is needed to mitigate adverse effects and maximize the climate-resilience of high-latitude cities. Studies that also consider the morphology of urban districts or neighborhoods like building-height-to-street-width ratios, building patterns, shapes, and orientation should be conducted.

CRediT authorship contribution statement

J. Brozovsky: Conceptualization, Data curation, Investigation, Methodology, Formal analysis, Software, Validation, Project administration, Writing - original draft, Writing - review & editing. **S. Corio:** Formal analysis, Investigation, Software, Validation, Visualization, Writing - review & editing. **N. Gaitani:** Conceptualization, Methodology, Writing - review & editing. **A. Gustavsen:** Conceptualization, Methodology, Supervision.

Declaration of Competing Interest

The authors declare that they have no known competing financial interests or personal relationships that could have appeared to influence the work reported in this paper.

Acknowledgments

This paper has been written within the Research Centre on Zero Emission Neighbourhoods in Smart Cities (FME ZEN). The authors gratefully acknowledge the support from the ZEN partners and the Research Council of Norway.

References

[1] L. Howard, The Climate of London Deduced From Meteorological Observations Made in the Metropolis and at Various Places Around It, 2nd ed., Harvey and Darton; J. Rickerby, London, 1833.
[2] United Nations, Department of Economic and Social Affairs, Population Division. World Urbanization Prospects: The 2018 Revision. Online Edition. New York, USA; 2018.
[3] O. Edenhofer (Ed.), Climate change 2014: Mitigation of climate change Working Group III contribution to the Fifth Assessment Report of the Intergovernmental Panel on Climate Change, Cambridge University Press, New York (USA), 2014.
[4] G. Mills, Urban climatology: history, status and prospects, Urban Clim. 10 (2014) 479–489, https://doi.org/10.1016/j.uclim.2014.06.004.
[5] T.R. Oke, Urban heat islands, in: I. Douglas, D. Goode, M. Houck, D. Maddox (Eds.), The Routledge Handbook of Urban Ecology, 1st ed., Routledge, London, 2011, pp. 120–131.
[6] I.D. Stewart, T.R. Oke, Local climate zones for urban temperature studies, Bull. Am. Meteor. Soc. 93 (12) (2012) 1879–1900, https://doi.org/10.1175/BAMS-D-11-00019.1.
[7] J. Berko, D.D. Ingram, S. Saha, J.D. Parker, Deaths Attributed to Heat, Cold and Other Weather Events in the United States, 2006–2010, Hyattsville, MD, USA, 2014.
[8] A. Fouillet, G. Rey, F. Laurent, G. Pavillon, S. Bellec, C. Guihenneuc-Jouyaux, et al., Excess mortality related to the August 2003 heat wave in France, Int. Arch. Occup. Environ. Health 80 (1) (2006) 16–24, https://doi.org/10.1007/s00420-006-0089-4.
[9] D. Shaposhnikov, B. Revich, T. Bellander, G.B. Bedada, M. Bottai, T. Kharkova, et al., Mortality related to air pollution with the moscow heat wave and wildfire of 2010, Epidemiology (Cambridge, Mass.) 25 (3) (2014) 359–364, https://doi.org/10.1097/EDE.0s000000000000090.
[10] M.S. O'Neill, K.L. Ebi, Temperature extremes and health: impacts of climate variability and change in the United States, J. Occup. Environ. Med. 51 (1) (2009) 13–25, https://doi.org/10.1097/JOM.0b013e318173e122.
[11] T.R. Oke, G. Mills, A. Christen, J.A. Voogt, Urban Climates, Cambridge University Press, Cambridge, 2017.
[12] H. Akbari, Shade trees reduce building energy use and CO2 emissions from power plants, Environ. Pollut. 116 (2002) S119–S126, https://doi.org/10.1016/S0269-7491(01)00264-0.
[13] D.E. Bowler, L. Buyung-Ali, T.M. Knight, A.S. Pullin, Urban greening to cool towns and cities: a systematic review of the empirical evidence, Landsc Urban Plan 97 (3) (2010) 147–155, https://doi.org/10.1016/j.landurbplan.2010.05.006.
[14] C.-R. Chang, M.-H. Li, Effects of urban parks on the local urban thermal environment, Urban Urban Green 13 (4) (2014) 672–681, https://doi.org/10.1016/j.ufug.2014.08.001.
[15] N.J. Georgi, K. Zafiriadis, The impact of park trees on microclimate in urban areas, Urban Ecosyst. 9 (3) (2006) 195–209, https://doi.org/10.1007/s11252-006-8590-9.
[16] C.-M. Hsieh, J.-J. Li, L. Zhang, B. Schwegler, Effects of tree shading and transpiration on building cooling energy use, Energy Build. 159 (2018) 382–397, https://doi.org/10.1016/j.enbuild.2017.10.045.
[17] H. Yan, F. Wu, L. Dong, Influence of a large urban park on the local urban thermal environment, Sci. Total Environ. 622–623 (2018) 882–891, https://doi.org/10.1016/j.scitotenv.2017.11.327.
[18] E.G. McPherson, J.R. Simpson, Potential energy savings in buildings by an urban tree planting programme in California, Urban Urban Green 2 (2) (2003) 73–86, https://doi.org/10.1078/1618-8667-00025.
[19] H. Jin, T. Shao, R. Zhang, Effect of water body forms on microclimate of residential district, Energy Proc. 134 (2017) 256–265, https://doi.org/10.1016/j.egypro.2017.09.615.
[20] H. Akbari, S. Menon, A. Rosenfeld, Global cooling: increasing world-wide urban albedos to offset CO2, Clim. Change 94 (3–4) (2009) 275–286, https://doi.org/10.1007/s10584-008-9515-9.
[21] H. Akbari, M. Pomerantz, H. Taha, Cool surfaces and shade trees to reduce energy use and improve air quality in urban areas, Sol Energy 70 (3) (2001) 295–310, https://doi.org/10.1016/S0038-092X(00)00089-X.
[22] L. Doulos, M. Santamouris, I. Livada, Passive cooling of outdoor urban spaces. The role of materials, Sol. Energy 77 (2) (2004) 231–249, https://doi.org/10.1016/j.solener.2004.04.005.
[23] A. Mohajerani, J. Bakaric, T. Jeffrey-Bailey, The urban heat island effect, its causes, and mitigation, with reference to the thermal properties of asphalt concrete, J. Environ. Manage. 197 (2017) 522–538, https://doi.org/10.1016/j.jenvman.2017.03.095.
[24] P. Savio, C. Rosenzweig, W.D. Solecki, R.B. Slosberg. Mitigating New York City's Heat Island with Urban Forestry, Living Roofs, and Light Surfaces: New York City Regional Heat Island Initiative; 2006.
[25] M.Z. Jacobson, J.E. ten Hoeve, Effects of urban surfaces and white roofs on global and regional climate, J. Clim. 25 (3) (2012) 1028–1044, https://doi.org/10.1175/JCLI-D-11-00032.1.
[26] F. Salata, I. Golasi, Ad.L. Vollaro, Rd.L. Vollaro, How high albedo and traditional buildings' materials and vegetation affect the quality of urban microclimate. A case study, Energy Build. 99 (2015) 32–49, https://doi.org/10.1016/j.enbuild.2015.04.010.
[27] Y. Wang, H. Akbari, Analysis of urban heat island phenomenon and mitigation solutions evaluation for Montreal, Sustain. Cities Soc. 26 (2016) 438–446, https://doi.org/10.1016/j.scs.2016.04.015.
[28] A.G. Touchaei, H. Akbari, Evaluation of the seasonal effect of increasing albedo on urban climate and energy consumption of buildings in Montreal, Urban Clim. 14 (2015) 278–289, https://doi.org/10.1016/j.uclim.2015.09.007.
[29] Y. Wang, U. Berardi, H. Akbari, Comparing the effects of urban heat island mitigation strategies for Toronto, Canada, Energy Build. 114 (2016) 2–19, https://doi.org/10.1016/j.enbuild.2015.06.046.
[30] B. Chun, J.-M. Guldmann, Impact of greening on the urban heat island: seasonal variations and mitigation strategies, Comput. Environ. Urban 71 (2018) 165–176, https://doi.org/10.1016/j.compenvurbsys.2018.05.006.
[31] S.A. Lowe, An energy and mortality impact assessment of the urban heat island in the US, Environ. Impact Assess Rev. 56 (2016) 139–144, https://doi.org/10.1016/j.eiar.2015.10.004.
[32] V.V. Klimenko, A.S. Ginzburg, P.F. Demchenko, A.G. Tereshin, I.N. Belova, E.V. Kasilova, Impact of urbanization and climate warming on energy consumption in large cities, Dokl Phys. 61 (10) (2016) 521–525, https://doi.org/10.1134/S1028335816100050.

[33] M. Varentsov, P. Konstantinov, A. Baklanov, I. Esau, V. Miles, R. Davy, Anthropogenic and natural drivers of a strong winter urban heat island in a typical Arctic city, Atmos. Chem. Phys. Discuss. (2018) 1–28, https://doi.org/10.5194/acp-2018-569.
[34] M. Półrolniczak, L. Kolendowicz, A. Majkowska, B. Czernecki, The influence of atmospheric circulation on the intensity of urban heat island and urban cold island in Poznań, Poland, Theor. Appl. Climatol. 127 (3–4) (2017) 611–625, https://doi.org/10.1007/s00704-015-1654-0.
[35] P. Konstantinov, M. Varentsov, I. Esau, A high density urban temperature network deployed in several cities of Eurasian Arctic, Environ. Res. Lett. 13 (7) (2018) 75007, https://doi.org/10.1088/1748-9326/aacb84.
[36] S.-H. Lee, J.-J. Baik, Statistical and dynamical characteristics of the urban heat island intensity in Seoul, Theor. Appl. Climatol. 100 (1–2) (2010) 227–237, https://doi.org/10.1007/s00704-009-0247-1.
[37] M.N. Khaikine, I.N. Kuznetsova, E.N. Kadygrov, E.A. Miller, Investigation of temporal-spatial parameters of an urban heat island on the basis of passive microwave remote sensing, Theor. Appl. Climatol. 84 (1–3) (2006) 161–169, https://doi.org/10.1007/s00704-005-0154-z.
[38] M. Stopa-Boryczka, J. Boryczka, J. Wawer, Impact of build-up areas and housing estate vegetation on diversity of the local climate in Warsaw, Misc. Geogr. 14 (1) (2010) 121–134, https://doi.org/10.2478/mgrsd-2010-0012.
[39] Y.-H. Kim, J.-J. Baik, Spatial and temporal structure of the urban heat island in Seoul, J. Appl. Meteorol. 44 (2005) 591–605.
[40] K.M. Hinkel, F.E. Nelson, A.E. Klene, J.H. Bell, The urban heat island in winter at Barrow, Alaska, Int. J. Climatol. 23 (15) (2003) 1889–1905, https://doi.org/10.1002/joc.971.
[41] V. Miles, I. Esau, Seasonal and spatial characteristics of Urban Heat Islands (UHIs) in Northern West Siberian Cities, Remote Sens. 9 (10) (2017) 989, https://doi.org/10.3390/rs9100989.
[42] J. Suomi, J. Käyhkö, The impact of environmental factors on urban temperature variability in the coastal city of Turku, SW Finland, Int. J. Climatol. 32 (3) (2012) 451–463, https://doi.org/10.1002/joc.2277.
[43] J. Schatz, C.J. Kucharik, Seasonality of the Urban Heat Island Effect in Madison, Wisconsin, J. Appl. Meteorol. Climatol. 53 (10) (2014) 2371–2386, https://doi.org/10.1175/JAMC-D-14-0107.1.
[44] P. Karsisto, C. Fortelius, M. Demuzere, C.S.B. Grimmond, K.W. Oleson, R. Kouznetsov, et al., Seasonal surface urban energy balance and wintertime stability simulated using three land-surface models in the high-latitude city Helsinki, Q. J. Roy Meteorol. Soc. 142 (694) (2016) 401–417, https://doi.org/10.1002/qj.2659.
[45] A. Semádeni-Davies, L. Bengtsson, Snowmelt sensitivity to radiation in the urban environment, Hydrol. Sci. J. 43 (1) (1998) 67–89, https://doi.org/10.1080/02626669809492103.
[46] S.A. Bowling, C.S. Benson, Study of the subarctic heat island at fairbanks, Alaska (1978).
[47] G.G. Aleksandrov, I.N. Belova, A.S. Ginzburg, Anthropogenic heat flows in the capital agglomerations of Russia and China, Dokl Earth Sci. 457 (1) (2014) 850–854, https://doi.org/10.1134/S1028334X14070010.
[48] I. Esau, V. Miles, M. Varentsov, P. Konstantinov, V. Melnikov, Spatial structure and temporal variability of a surface urban heat island in cold continental climate, Theor. Appl. Climatol. 31 (12) (2019) 1990, https://doi.org/10.1007/s00704-018-02754-z.
[49] K.M. Hinkel, F.E. Nelson, Anthropogenic heat island at Barrow, Alaska, during winter: 2001–2005, J. Geophys. Res. 112 (D6) (2007) 1, https://doi.org/10.1029/2006JD007837.
[50] Y. Toparlar, B. Blocken, B. Maiheu, G.J.F. van Heijst, A review on the CFD analysis of urban microclimate, Renew Sustain. Energy Rev. 80 (2017) 1613–1640, https://doi.org/10.1016/j.rser.2017.05.248.
[51] T. Heleniak, The future of the Arctic populations, Polar Geogr. (2020) 1–17, https://doi.org/10.1080/1088937X.2019.1707316.
[52] T. Heleniak, S. Wang, E. Turunen. Cities on Ice: Population change in the Arctic; Available from: http://www.nordregio.org/nordregio-magazine/issues/arctic-changes-and-challenges/cities-on-ice-population-change-in-the-arctic/.
[53] K.G. Hansen, R.O. Rasmussen, R. Weber. Proceedings from the First International Conference on Urbanisation in the Arctic; 2013.
[54] L. Dicks, Arctic climate issues 2011: Changes in Arctic snow, water, ice and permafrost, Arctic Monitoring and Assessment Programme; Canadian Electronic Library, Oslo, Norway, Ottawa, Ontario, 2013.
[55] R.B. Jackson, P. Friedlingstein, R.M. Andrew, J.G. Canadell, C. Le Quéré, G.P. Peters, Persistent fossil fuel growth threatens the Paris Agreement and planetary health, Environ. Res. Lett. 14 (12) (2019), https://doi.org/10.1088/1748-9326/ab57b3 121001.
[56] R.K. Pachauri, L. Mayer (eds.). Climate change 2014: Synthesis report. Geneva, Switzerland: Intergovernmental Panel on Climate Change; 2015.
[57] D. Chapman, K. Nilsson, A. Larsson, A. Rizzo, Climatic barriers to soft-mobility in winter: Luleå, Sweden as case study, Sustain. Cities Soc. 35 (2017) 574–580, https://doi.org/10.1016/j.scs.2017.09.003.
[58] E. Erell, D. Pearlmutter, T. Williamson, Urban Microclimate: Designing the Spaces Between Buildings, Earthscan, London, 2011.
[59] Cambridge University Press. Cambridge Dictionary: English Dictionary. [April 23, 2020]; Available from: https://dictionary.cambridge.org/dictionary/english/.
[60] M. Xu, B. Hong, J. Mi, S. Yan, Outdoor thermal comfort in an urban park during winter in cold regions of China, Sustain. Cities Soc. 43 (2018) 208–220, https://doi.org/10.1016/j.scs.2018.08.034.
[61] W. Liu, Y. Zhang, Q. Deng, The effects of urban microclimate on outdoor thermal sensation and neutral temperature in hot-summer and cold-winter climate, Energy Build. 128 (2016) 190–197, https://doi.org/10.1016/j.enbuild.2016.06.086.
[62] X. Chen, L. Gao, P. Xue, J. Du, J. Liu, Investigation of outdoor thermal sensation and comfort evaluation methods in severe cold area, Sci. Total Environ. 749 (2020), https://doi.org/10.1016/j.scitotenv.2020.141520 141520.
[63] M. Nikolopoulou, S. Lykoudis, Thermal comfort in outdoor urban spaces: analysis across different European countries, Build. Environ. 41 (11) (2006) 1455–1470, https://doi.org/10.1016/j.buildenv.2005.05.031.
[64] B. Yang, T. Olofsson, G. Nair, A. Kabanshi, Outdoor thermal comfort under subarctic climate of north Sweden – A pilot study in Umeå, Sustain. Cities Soc. 28 (2017) 387–397, https://doi.org/10.1016/j.scs.2016.10.011.
[65] T. Stathopoulos, H. Wu, J. Zacharias, Outdoor human comfort in an urban climate, Build. Environ. 39 (3) (2004) 297–305, https://doi.org/10.1016/j.buildenv.2003.09.001.
[66] D. Lai, D. Guo, Y. Hou, C. Lin, Q. Chen, Studies of outdoor thermal comfort in northern China, Build. Environ. 77 (2014) 110–118, https://doi.org/10.1016/j.buildenv.2014.03.026.
[67] L. Chen, E. Ng, Outdoor thermal comfort and outdoor activities: A review of research in the past decade, Cities 29 (2) (2012) 118–125, https://doi.org/10.1016/j.cities.2011.08.006.
[68] L. Rui, R. Buccolieri, Z. Gao, E. Gatto, W. Ding, Study of the effect of green quantity and structure on thermal comfort and air quality in an urban-like residential district by ENVI-met modelling, Build. Simul. 12 (2) (2019) 183–194, https://doi.org/10.1007/s12273-018-0498-9.
[69] I. Karakounos, A. Dimoudi, S. Zoras, The influence of bioclimatic urban redevelopment on outdoor thermal comfort, Energy Build. 158 (2018) 1266–1274, https://doi.org/10.1016/j.enbuild.2017.11.035.
[70] A. Qaid, H. Bin Lamit, D.R. Ossen, R.N. Raja Shahminan, Urban heat island and thermal comfort conditions at micro-climate scale in a tropical planned city, Energy Build. 133 (2016) 577–595, https://doi.org/10.1016/j.enbuild.2016.10.006.
[71] M. Taleghani, L. Kleerekoper, M. Tenpierik, A. van den Dobbelsteen, Outdoor thermal comfort within five different urban forms in the Netherlands, Build. Environ. 83 (2015) 65–78, https://doi.org/10.1016/j.buildenv.2014.03.014.
[72] M. Taleghani, U. Berardi, The effect of pavement characteristics on pedestrians‘ thermal comfort in Toronto, Urban Clim. 24 (2018) 449–459, https://doi.org/10.1016/j.uclim.2017.05.007.
[73] U. Berardi, Y. Wang, The effect of a denser city over the urban microclimate: the case of toronto, Sustainability 8 (8) (2016) 822, https://doi.org/10.3390/su8080822.
[74] E. Gatto, R. Buccolieri, E. Aarrevaara, F. Ippolito, R. Emmanuel, L. Perronace, et al., Impact of urban vegetation on outdoor thermal comfort: comparison between a Mediterranean City (Lecce, Italy) and a Northern European City (Lahti, Finland), Forests 11 (2) (2020) 228, https://doi.org/10.3390/f11020228.
[75] E. Lundstad, O.E. Tveito. Homogenization of daily mean temperature in Norway; 2016.
[76] Meteorologisk Institutt. eKlima: Free access to weather- and climate data from Norwegian Meteorological Institute from historical data to real time observations. Normals; Available from: http://sharki.oslo.dnmi.no/portal/page?_pageid=73,39035,73_39049&_dad=portal&_schema=PORTAL.
[77] W.L. Oberkampf, T.G. Trucano, Verification and validation in computational fluid dynamics, Prog. Aerosp. Sci. 38 (2002) 209–272.
[78] American Institute of Aeronautics and Astronautics (ed.). 43rd AIAA Aerospace Sciences Meeting and Exhibit. Reston, Virigina: American Institute of Aeronautics and Astronautics; 2005.
[79] M. Bruse, H. Fleer, Simulating surface–plant–air interactions inside urban environments with a three dimensional numerical model, Environ. Model Softw. 13 (3–4) (1998) 373–384, https://doi.org/10.1016/S1364-8152(98)00042-5.
[80] M. Srivanit, K. Hokao, Evaluating the cooling effects of greening for improving the outdoor thermal environment at an institutional campus in the summer, Build. Environ. 66 (2013) 158–172, https://doi.org/10.1016/j.buildenv.2013.04.012.
[81] M.F. Shahidan, P.J. Jones, J. Gwilliam, E. Salleh, An evaluation of outdoor and building environment cooling achieved through combination modification of trees with ground materials, Build. Environ. 58 (2012) 245–257, https://doi.org/10.1016/j.buildenv.2012.07.012.
[82] W.T.L. Chow, A.J. Brazel, Assessing xeriscaping as a sustainable heat island mitigation approach for a desert city, Build. Environ. 47 (2012) 170–181, https://doi.org/10.1016/j.buildenv.2011.07.027.
[83] E. Carnielo, M. Zinzi, Optical and thermal characterisation of cool asphalts to mitigate urban temperatures and building cooling demand, Build. Environ. 60 (2013) 56–65, https://doi.org/10.1016/j.buildenv.2012.11.004.
[84] H. Lee, H. Mayer, L. Chen, Contribution of trees and grasslands to the mitigation of human heat stress in a residential district of Freiburg, Southwest Germany, Landsc Urban Plan 148 (2016) 37–50, https://doi.org/10.1016/j.landurbplan.2015.12.004.
[85] M. Taleghani, D.J. Sailor, M. Tenpierik, A. van den Dobbelsteen, Thermal assessment of heat mitigation strategies: the case of Portland State University, Oregon, USA, Build. Environ. 73 (2014) 138–150, https://doi.org/10.1016/j.buildenv.2013.12.006.

[86] S.B. Malevich, K. Klink, Relationships between Snow and the Wintertime Minneapolis Urban Heat Island, J. Appl. Meteorol. Climatol. 50 (9) (2011) 1884–1894, https://doi.org/10.1175/JAMC-D-11-05.1.
[87] E.M.O. Sigmond, Nasjonalatlas for Norge: National atlas of Norway, Statens kartverk, Oslo, 1985.
[88] ENVI_MET GmbH. ENVI_MET V4.4.2: Winter1819. Essen, Germany; 2019.
[89] M. Santamouris (Ed.), Environmental design of urban buildings: An integrated approach, Earthscan, London, 2006.
[90] A. Goris, K.-J. Schneider, A. Albert (Eds.), Bautabellen für Ingenieure: Mit Berechnungshinweisen und Beispielen, 19th ed., Neuwied, Köln, Werner; Wolters Kluwer, 2010.
[91] M. Schatzmann, B. Leitl, Issues with validation of urban flow and dispersion CFD models, J. Wind Eng. Ind. Aerodyn. 99 (4) (2011) 169–186, https://doi.org/10.1016/j.jweia.2011.01.005.
[92] S. Imam, D.A. Coley, I. Walker, The building performance gap: are modellers literate?, Build Serv. Eng. Res. T 38 (3) (2017) 351–375, https://doi.org/10.1177/0143624416684641.
[93] A. Skartveit, J.A. Olseth, A model for the diffuse fraction of hourly global radiation, Sol Energy 38 (4) (1987) 271–274.
[94] P.O. Fanger, Thermal Comfort: Analysis and Applications in Environmental Engineering, Danish Technical Pr, Copenhagen, 1970.
[95] G. Jendritzky, W. Nübler, A model analysing the urban thermal environment in physiologically significant terms, Arch. Met. Geoph. Biokl. B 29 (4) (1981) 313–326.
[96] Association of German Engineers. VDI 3787 Part 2: Environmental meteorology - Methods for the human biometeorological evaluation of climate and air quality for urban and regional planning at regional level; 2008.
[97] F. Salata, I. Golasi, R. de Lieto Vollaro, Lieto Vollaro A de. Urban microclimate and outdoor thermal comfort. A proper procedure to fit ENVI-met simulation outputs to experimental data, Sustain. Cities Soc. 26 (2016) 318–343, https://doi.org/10.1016/j.scs.2016.07.005.
[98] Alemu M. Mekonnen, Ecological benefits of trees as Windbreaks, Int. J. Ecosyst. 6 (1) (2016) 10–13.
[99] H. Leng, S. Liang, Q. Yuan, Outdoor thermal comfort and adaptive behaviors in the residential public open spaces of winter cities during the marginal season, Int. J. Biometeorol. 64 (2) (2020) 217–229, https://doi.org/10.1007/s00484-019-01709-x.
[100] E. Jamei, P. Rajagopalan, M. Seyedmahmoudian, Y. Jamei, Review on the impact of urban geometry and pedestrian level greening on outdoor thermal comfort, Renew. Sustain. Energy Rev. 54 (2016) 1002–1017, https://doi.org/10.1016/j.rser.2015.10.104.